fibers

MDPI

Article

Use of Ginger Nanofibers for the Preparation of Cellulose Nanocomposites and Their Antimicrobial Activities

Joby Jacob [1], Józef T. Haponiuk [2], Sabu Thomas [3], Gregary Peter [1] and Sreeraj Gopi [1,*]

[1] R&D Centre, Aurea Biolabs (P) Ltd., Kolenchery, Cochin 682311, Kerala, India; joby.jacob@plantlipids.com (J.J.); sreejith.mohan@plantlipids.com (G.P.)
[2] Department of Polymer Technology, Gdansk University of Technology, 80-233 Gdańsk, Poland; jozef.haponiuk@pg.edu.pl
[3] School of Chemical Sciences, Mahatma Gandhi University, Kottayam 686560, Kerala, India; sabupolymer@yahoo.com
* Correspondence: sreeraj.gopi@plantlipids.com; Tel.: +91-484-305-1500

Received: 11 September 2018; Accepted: 2 October 2018; Published: 15 October 2018

Abstract: Ginger residues left after the extraction of active ingredients from ginger rhizomes are considered to be a bio-waste, available in abundance and very rarely used. Extraction and isolation of natural nanofibers from the agro-waste is economical, environmentally benign, and an alternate strategy to replace synthetic fibers. Here, we report, for the first time, the isolation of ginger nanofibers (GNF) from ginger rhizomes spent by acid hydrolysis and followed by high-pressure homogenization. Scanning electron microscopy was utilized to identify the surface morphology of the GNF and the widths ranged between 130 to 200 nm. Structural analysis of GNF was identified by Fourier transform infrared spectroscopy, Differential scanning calorimetry, and X-ray diffraction methods. This GNF was used to make natural nanocomposites by the solvent-casting method reinforcement, using potato starch (PS) and tapioca starch (TS), and was characterized through various methods. These composites were prepared by the addition of 1, 3, 5, and 7 weight % of GNF with PS or TS. Among these, 5% of the GNF composites of these starches showed very high mechanical properties. The antibacterial test showed that the bionanocomposites with 5% GNF exhibited good antibacterial activity against *Bacillus cereus*, *Escherichia coli*, *Staphylococcus aureus*, and *Salmonella typhimurium*, due to the addition of GNF in the biopolymer matrices. The viable use of GNF from the unexploited ginger agro-waste would create additional profit and it would help to diminish a large amount of waste generation. Thus, the developed bio-composite could also be employed for development of packing materials and be used in medical applications, such as wound healing pads and medical disposables.

Keywords: ginger nanofiber; starch; bionanocomposites; antimicrobial activity

1. Introduction

Synthetic polymers play an important role in modern research but the accumulation of non-degradable waste is a major environmental concern [1]. Nanocomposites prepared by biopolymers, such as cellulose and starch, attain much attention nowadays due to their versatile applications [2]. These biopolymers are abundant in nature, renewable, sustainable, and economical, when compared with synthetic fibers, and are an alternative to non-degradable synthetic ones [3]. Starch-based nanocomposites, cross-linked with cellulose nanofiber (CNF), would increase the mechanical and barrier properties of starch which could be prepared from biomass residues, hence they could be potential alternatives for fossil fuel-derived plastics, thus minimizing the creation of waste [4,5].

CNF can be isolated from biomass through acid hydrolysis, using a strong acid, like H_2SO_4 or HCl. CNF have unique properties, such as toughness, thickness, length, and their crystalline realm is well oriented, which helps to make more-resistant materials with distinct magnetic, optical, electrical, and conductivity properties, as compared to the macroscopic material [6–8]. There are many lignocellulosic sources available to make CNF, such as wood, cotton, jute, and many more [9]. Similarly, CNF isolated from turmeric agro-industrial waste have also been utilized in different applications, such as phytogenic feed additive [10], anti-colitis activity product [11], making bioavailable forms of curcumin [12,13], and liposomal powders [14]. These CNF have characteristic mechanical properties due to its ability to make chemical configurations through strong interactions and H-bonding, when mixed with starch [15,16]. The agricultural wastes can be utilized to make value-added products that make an extra income for farmers and lower the environmental pollution. CNF has captured widened interest, recently, in the field of pharmacology and medicinal applications because of their boundless potential to improve the functional qualities of drug delivery and antimicrobial action [17,18].

India is the largest producer of ginger rhizomes, estimated to be approximately 0.68 million tons, which account for 33% of the total world production [19]. A large amount of biomass is accumulated after the isolation of the oil and oleoresin. The generation of CNF from the ginger residue helps to reduce the agro-waste accumulation in the environment by diminishing the amount of waste generation and thus creates an additional profit. However, there has yet been no research done on the isolation of GNF from the ginger agro-residues.

Starch is composed of D-glucose derived linear amylose and branched amylopectin and can be isolated from various sources, such as wheat, corn, potato, and tapioca. Starch can be easily transformed to thermoplastic starch, which is a continuous phase as its granular structure is obtained during its biosynthesis [20]. Thermoplastic property of starch can be improved, significantly, by making composites, by the addition of plasticizers, such as water, glycerol, and sorbitol, with the help of thermal/or mechanical energy [21]. Even though these thermoplastic starches have improved free volume properties, yet they show some limitations, like low-mechanical properties and high affinity towards water, hence, they are strongly affected by relative humidity [22]. Addition of cellulose nanofibers (CNF) to the starch helps to overcome these hurdles and offers a promising strategy. These biocomposites display low toxicity, biodegradability, high tensile strength, flexibility, and thermal stability [23]. Moreover, these CNF have many applications in the production of cellulose-based nanomaterials which have potential uses in different fields, such biomedicine [24], drug delivery systems [2], textiles [25], as coating materials [26], and in paper production [27].

In the present study, we prepared ginger nanofibers (GNF)—the first attempt to do this from ginger waste after the extraction of active ingredients, like gingerols and shogaol—and used them to make composites, with potato starch (PS) or tapioca starch (TS), through the solvent-casting method. Due to the high availability and low cost, we chose PS and TS-based thermoplastic starch as the plasticizers for the GNF, to make the composites. We used four different compositions viz. 1%, 3%, 5%, and 7% of the GNF, to reinforce the composite with the PS and TS. Ginger contains approximately 3% of fiber and the NF isolated from ginger could be a promising approach, as it has distinctive chemical properties and pronounced biological activities. These GNF have been characterized through various methods, such as Fourier transform infrared spectroscopy (FT-IR), scanning electron microscopy (SEM), X-ray diffraction (XRD), and differential scanning colorimetry (DSC). In addition, the antibacterial activities of GNF, as well as nanocomposite films, were evaluated against that of the *Bacillus cereus*, *Escherichia coli*, *Staphylococcus aureus*, and *Salmonella typhimurium*. The antibacterial activities of these composites were confirmed against, both, Gram-positive-and-negative bacterial pathogens.

2. Materials and Methods

2.1. Isolation of Ginger Nanofiber (GNF)

Ginger spent was obtained from Plant Lipids (P) Ltd., Kerala, India after the isolation of natural ingredients, such as gingerols and shogaol. The powdered ginger agro-waste was washed with distilled water to remove dirt, dust, and water-soluble impurities. Then the ginger spent was dried before the isolation of GNF, which was produced as per the protocol described earlier, with some modifications [28]. Cleaned ginger residues were treated with 4% NaOH solution (*w*/*w*) at 80 °C, for 2 h, under mechanical stirring which removed the residual additives, such as partially solubilized pectin, lignin, and hemicellulose impurities. After each treatment, the obtained reaction mass was filtered and washed with distilled water, until the filtrate became neutral. After this alkali treatment, the fiber was decolorized with aqueous 3% sodium chlorite (*w*/*w*) to bleach and leach the fiber. This process was accomplished at 80 °C, for 2 h, and was repeated two times. The resultant fiber was washed continuously in distilled water, until the complete removal of sodium chlorite. After this, the residue was hydrolyzed using 10% H_2SO_4 (*w*/*w*), at 80 °C, for 2 h, using mechanical stirring. The acid hydrolysis treatment helped in leaching out traces of minerals, residual starch, and also hydrolyzed amorphous cellulose and eased in getting the required fiber suspension. After the acid hydrolysis, the reaction mass was cooled with ice cubes to quench the hydrolysis, washed with distilled water, and centrifuged for 20 min, at 8000 rpm, at 10 °C. The resulted suspension was homogenized using APV 1000 homogenizer (SPX Flow Technology, Holzwickede, Germany) with five passes, with an operating pressure of 1000 bar, and filtered using a glass filter to obtain the GNF. The GNF solution was concentrated to near 2–3% (by weight) dispersion and kept under refrigeration to make composites.

2.2. Preparation of Bionanocomposites

The solvent-casting method was used to prepare the bionanocomposites, as reported earlier with some variations [28]. The known weight of GNF was suspended in 100 mL distilled water, under stirring for 30 min, then sonicated for 20 min, using an ultrasonic bath sonicator (PCI Analytics Pvt. Ltd., Mumbai, India). The obtained GNF suspension was stirred well with formerly prepared PS/TS with glycerol (15 weight % on dry basis), in 100 mL water, for 30 min, at 80 °C, to get a homogenous suspension. The resulting solution was sonicated for 20 min, and approximately 100 mL of solution was carefully poured on to a Borosil petri dish, to get an even thickness. The plates were kept at 55–60 °C, for 12 h, till it dried completely. 1, 3, 5, and 7 weight % of GNF were used to prepare these films of potato starch–ginger nanofiber (PS–GNF) and tapioca starch–ginger nanofiber (TS–GNF).

2.3. Characterization and Measurement of the GNF and Bionanocomposites

2.3.1. Fourier Transform Infrared Spectroscopy (FTIR-ATR)

FTIR-ATR spectra were recorded using a JASCO ATR-FT/IT-4700 instrument. All the samples were dried well and analyzed at a range of 400–4000 cm^{-1}, with 32 scans per sample.

2.3.2. Scanning Electron Microscopy (SEM)

The surface morphology of the GNF and composites samples were examined using a scanning electron microscope (Vega3 Tescan, Brno, Czech Republic). Prepared samples were placed in aluminum stubs with double-sided carbon tape and sputter-layered with a fine coating of gold, using a sputter gold coater to eliminate charring, during the analysis. Prepared GNF and bionanocomposites were scanned using an accelerating voltage of 20 kV.

2.3.3. X-ray Diffraction (XRD)

The crystalline properties of the GNF and the prepared bionanocomposites were determined by an X-ray diffractometer (Xpert-Pro). Oven dried samples were analyzed at ambient temperatures,

using Ni-filtered Cu K radiation (λ = 0.1541 nm), over the scattering 2θ angles from 5° to 80°, with a scanning speed of 1.2°/min.

2.3.4. Mechanical Test

The mechanical properties of the GNF and composites were determined using a Universal Test Machine (Tinius Olsen, H1KS Benchtop Tester, load cell of 1 kN, Noida, India) with a crosshead speed of 60 mm/min. All tests were conducted at room temperature till the elongation breakage happened. The films were cut into 0.1 × 5 × 40 mm^3 and the results were the average of five measurements, for each formulation.

2.3.5. Differential Scanning Calorimetry (DSC)

The thermal properties of the GNF and the prepared bionanocomposites films were estimated on a differential scanning calorimeter (DSC) Q10 DSC equipment (Mettler Toledo DSC 822e, Greifensee, Switzerland). About 5–7 mg of the film sample was weighed in an aluminum crucible and the reference was an empty aluminum crucible for all DSC analysis. The bionanocomposite films were heated from 0 to 400 °C, at a range of 10 °C /min, under a nitrogen flow of 10 mL/min.

2.4. Antimicrobial Activity

All the title compounds were screened for their in vitro antibacterial activity against four bacterial species as experiment organisms which include two gram-positive strains, i.e., *Bacillus cereus*, *Staphylococcus aureus*, and two gram-negative strains, i.e., *Escherichia coli*, and *Salmonella typhimurium*. The bacteria were preserved in Mueller Hinton Agar (MH). Inocula were prearranged through accumulation, during the night civilization of the organisms in the MH broth, to attain 0.1 OD_{600} suspension. The groups were permitted to cultivate until they attained the 0.5 McFarland turbidity standard (approximately, 1.5 × 108 CFU/mL). However, this concentration was further diluted to attain 106 CFU/mL (1:1000) in MH broth, for the determination of Minimum Inhibitory Concentration (MIC). The prepared GNF, PS–GNF, TS–GNF, and ampicillin disc (positive control) were positioned on the MH agar plates, earlier swabbed with the objective bacterial segregate, at a concentration of 106 CFU/mL. In a disc, the particular solvent was mixed as a negative control, to establish the probable inhibition activity of the solvent. Then it was isolated for a period of 24 h, at 30 °C. Antibacterial activity was defined as the diameter of the comprehensible inhibitory region formed around the discs.

3. Results and Discussions

3.1. Fourier Transform Infrared Spectroscopy (FTIR-ATR)

FT-IR spectra of individual starches, GNF, and bionanocomposites of PS–GNF (5% GNF) and TS–GNF (5% GNF) are shown in Figure 1. PS and TS showed almost a similar pattern and a very broad band appeared at 3427 cm^{-1}, due to the vibration of the H-bonded hydroxyl groups (O-H) [29]. The typical broad band at 3340 cm^{-1}, due to the -OH group stretching of the cellulose and it was decreased to 3298 cm^{-1}, in both GNF–PS and GNF–TS. This was due to the intermolecular hydrogen bonding between GNF and the starch matrices, which indicated the formation of bionancomposites [30,31]. The peak at 2900 cm^{-1} matched up with the C-H symmetrical stretching which indicated the existence of polysaccharide functionality, and was observed in all of the samples. The sharp peak at 1027 cm^{-1} represented the C-O-C and C-H vibrational stretching of cellulose. It indicated that the hemicellulose xylan, presented in the GNF, confirmed the higher cellulose content in the GNF [11]. The peak presented at 1446 cm^{-1} was attributed to the H-C-H in plane-bending vibrations. Moreover, the H-O-H bending of the absorbed water was detected at 1643 cm^{-1} which was larger in the GNF–PS than the GNF and GNF–TS, indicating that the GNF–PS was more hygroscopic

than GNF and GNF–TS [32]. This was further confirmed by the larger -OH stretching of the GNF–PS, at 3298 cm^{-1}, compared to the GNF–TS.

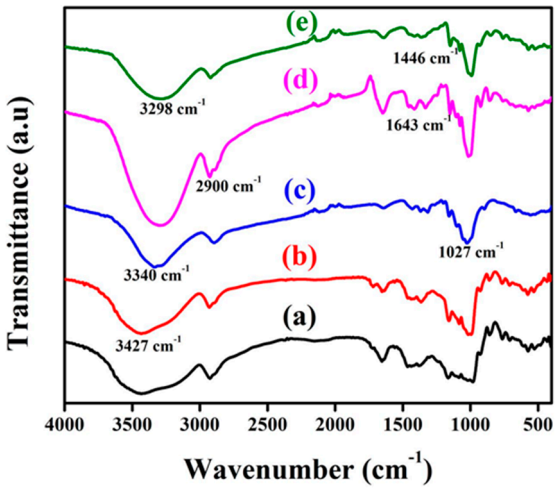

Figure 1. FTIR images of PS (**a**), TS (**b**), GNF (**c**), and 5% GNF with PS (**d**) and TS (**e**) composites.

3.2. Scanning Electron Micrograph (SEM)

The scanning electron micrographs of the GNF and the bionanocomposites of the PS–GNF and TS–GNF are shown in Figures 2 and 3. Figure 2a,b shows the morphological changes before and after the homogenization. The cellulose matrix was in a colloidal stage before homogenization was attributed to the hydrolysis of the matrix and after the homogenization, the width of the GNF decreased to 130 to 200 nm, as in the Figure 2b, which indicated that high pressure could reform the structural morphology of the cellulose.

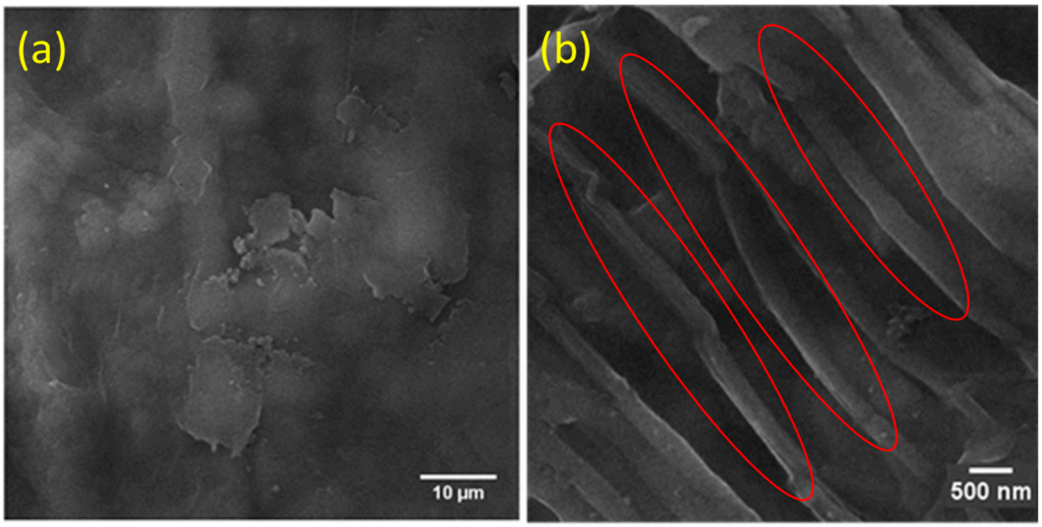

Figure 2. SEM images of the GNF before (**a**) and after (**b**) homogenization. (The formation of the GNF is marked in red).

Figure 3a,b show the SEM micrographs of the bionanocomposite films of the PS–GNF and TS–GNF, with 5 weight % of the GNF, respectively. A coarse and uneven morphology was obtained after the addition of the GNF in the PS and the TS, which resulted in tight and aggregated film matrices, due to the strong intermolecular H-bonding of the GNF with the starch matrices. The structured SEM micrographs of the composites indicated that the GNF uniformly dispersed in the PS and the TS matrices, due to the strong electrostatic interactions, along with H-bonding. In addition,

the incorporation of the GNF to the starch matrices resulted in higher density composite films, as indicated by the SEM images.

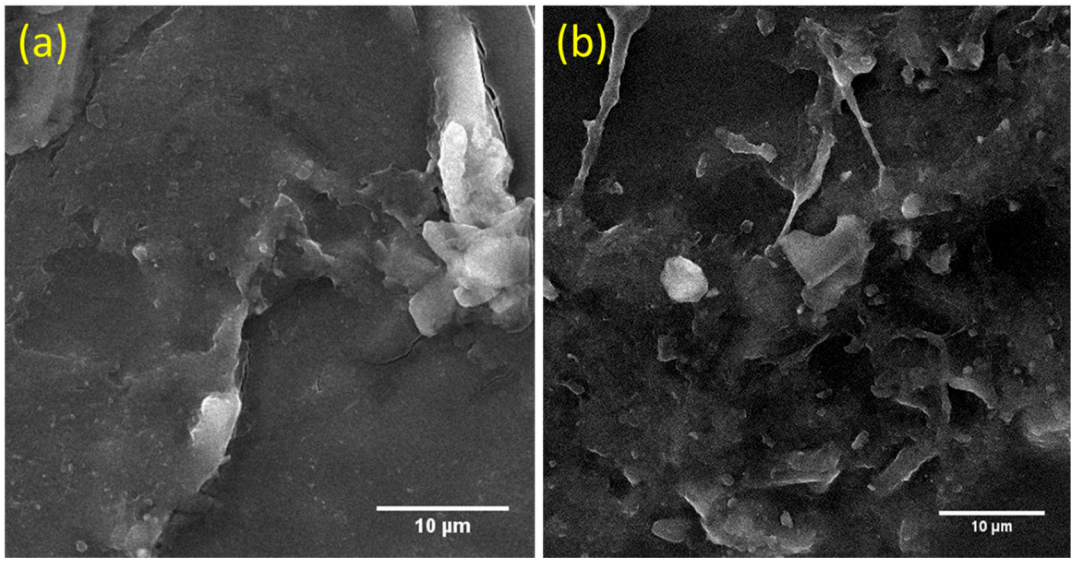

Figure 3. SEM images of the GNF (5%) with Potato starch (**a**) and Tapioca starch (**b**).

3.3. X-ray Diffraction (XRD)

The crystallinity of the GNF was the key feature to resolve the performance of the nanocomposites. Figure 4 illustrates the XRD diffractograms for the GNF and its bionanocomposites, with 5% GNF films using the PS and the TS. The characteristic peak for GNF 2θ, around 23°, was allotted to the cellulose crystalline structure. Strong inter and intramolecular interfaces resulted in the higher crystallinity of GNF achieved by the acid hydrolysis. Moreover, the two peaks at 2θ = 23° and 16° identified the existence of the orthorhombic cellulose crystal I and II. The crystalline nature of the GNF enhanced the rigidity and firmness of the composites, during the reinforcement [33]. The crystalline nature of the GNF was still preserved in the bionanocomposites, as the peak at 23° was still present in the nanocomposites, even though, the content of the GNF was low (5%).

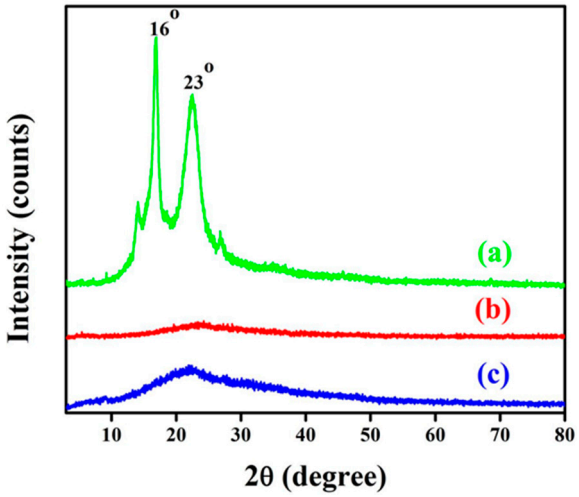

Figure 4. X-ray diffractograms of GNF (**a**) and composites with 5% GNF, composited with PS (**b**) and TS (**c**).

3.4. Mechanical Properties

The effects of GNF on tensile strength, and percent elongation at break and Young's modulus of starches and composite films are displayed in Table 1. The tensile strength of the composites was gradually increased from 100% PS film to 5% GNF–PS composite and the values were 1.6 and 3.9 MPa, respectively. The same trend was experienced in the GNF–TS as 2.3 MPa (TS alone) to 4.2 MPa (5% GNF–TS). The tensile strength further decreased in the 7% GNF composite for both PS (3.2 MPa) and TS (3.9 MPa), when compared to the 5% composites. This may be because the increase of the GNF led to the decrease in molecular mobility. This increased the stiffness of the starch composites, which made the composites more brittle. This further reduced the strain, at the break, and the flexural strength, with a higher GNF loading [34]. The elongation at the break reduced from of 61% (PS alone) to 44% (5% GNF–PS), then increased to 45% (7% GNF–PS). Similarly, for the TS, the elongation at the break decreased from 55% (TS alone) to 43% (5% GNF–TS), then increased to 44% (7% TS–GNF). Young's modulus also showed the same trend as the tensile strength, which increased up to the 5% GNF composite and decreased for the 7% GNF composites, in both the PS and the TS.

Table 1. Mechanical properties of the GNF–PS and GNF–TS composites with different compositions.

Sample	Tensile Strength (MPa)	Young's Modulus (MPa)	Elongation at Break (%)
PS	1.6 ± 0.6	19 ± 1	61 ± 2
GNF–PS (1%)	2.2 ± 0.5	22 ± 2	53 ± 1
GNF–PS (3%)	2.9 ± 1.2	24 ± 2	48 ± 2
GNF–PS (5%)	3.9 ± 0.9	32 ± 1	44 ± 1
GNF–PS (7%)	3.2 ± 0.9	29 ± 1	45 ± 2
TS	2.3 ± 0.8	22 ± 1	55 ± 2
GNF–TS (1%)	2.5 ± 0.3	25 ± 1	52 ± 2
GNF–TS (3%)	3.1 ± 0.8	29 ± 1	47 ± 2
GNF–TS (5%)	4.2 ± 0.4	33 ± 1	43 ± 2
GNF–TS (7%)	3.9 ± 0.7	29 ± 2	44 ± 2

The high tensile strength and low elongation at the break showed the good mechanical properties of the films. These results showed that the cross-linking of the GNF, with the PS and the TS, noticeably increased the tensile strength and the Young's modulus, until up to 5% addition of GNF and decreased at 7% addition of the GNF, as was expected. Similarly, the elongation at the break, decreased up to the addition of 5% GNF, showing that the mechanical properties were maximum at 5% of the GNF cross-linked with PS and TS. These modifications were associated with a solid interfacial interface comprising the GNF with the starch environment. This association was enabled by the prevailing strong intermolecular H-bonds (with hydrogen acceptors of polymer molecules) among the GNF cellulose [35], as well as the PS and the TS, The results were in good agreement with the FTIR results.

3.5. Thermal Properties by DSC

The DSC analysis of GNF and the bionanocomposite films reinforced with 5% of the GNF content are presented in Table 2 and the DSC curves are presented in Figure 5. The results were similar to the typical endothermic values which were attributable to the starch gelatinization. The onset temperature (T_{onset}) of GNF was 33 °C, the peak temperature (T_{peak}) was 69 °C, and endset temperature (T_{endset}) was 107 °C. These parameters were higher in the nanocomposites because of the stiffness of the composite films. This was caused by the well-ordered alignment of the GNF cellulose in the composite moiety. This alignment is as a result of the chemical interaction with the starch molecules, which resulted more from the thermal stability of the composites than that of the GNF alone. The melting enthalpy ($\Delta H_{melting}$) was mainly used to estimate the degree of crystallinity and the value was higher in the GNF (109 J/g) than in the GNF–PS (21 J/g) and the GNF–TS (25 J/g) composites, which indicated a decrease in the degree of crystallinity, as revealed by the XRD analysis [36].

Table 2. DSC analysis of the GNF and the 5% loaded-GNF–PS and GNF–TS.

Sample	T_o (°C)	T_p (°C)	T_e (°C)	ΔH_m (J/g)
GNF	33	69	107	109
GNF–PS	57	78	108	21
GNF–TS	44	81	147	25

T_o: T_{onset}, T_p: T_{peak}, T_e: T_{endset}; ΔH_m: $\Delta H_{melting}$.

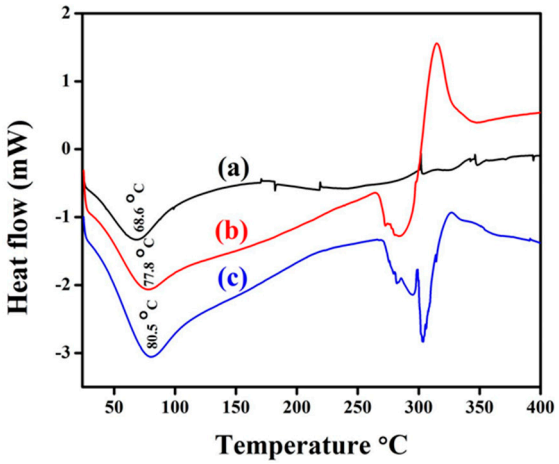

Figure 5. DSC curves of the GNF (**a**) and the 5% GNF-based nanocomposites, incorporated with PS (**b**) and TS (**c**).

3.6. Antibacterial Activities of Bionanocomposites

The minimum inhibitory concentration (MIC) of GNF, 5% GNF–PS, and 5% GNF–TS was determined by the agar diffusion assay, the results of which are shown in Table 3, along with the positive control (ampicillin). All tested strains were susceptible to the bionanocomposite films with variable degrees of MIC. The films were found effective against both gram-positive bacteria and gram-negative bacteria. The solvent control did not have any effect on the microorganism growth. In the case of the GNF film, the highest percentage of MIC value was observed, demonstrating that the GNF had maximum ability to inhibit the bacteria in the tested strains. Similarly, the prepared bionanocomposites (GNF–PS and the GNF–TS) were registered considerable inhibitory effect against the test organisms. Meanwhile, the MIC value of the GNF–TS film (8.3 ± 1 µg/mL against *Bacillus cereus*, 3.1 ± 0 µg/mL against *Escherichia coli*, 12 ± 2 µg/mL against *Staphylococcus aureus*, and 19 ± 1 µg/mL against *Salmonella typhimurium*) were slightly lower than those of the GNF–PS (9.1 ± 1 µg/mL against *Bacillus cereus*, 8.1 ± 1 µg/mL against *Escherichia coli*, 15 ± 1 µg/mL against *Staphylococcus aureus*, and 24 ± 2 µg/mL against *Salmonella typhimurium*). Additionally, the zone of inhibition by ampicillin, for the selected microorganisms, was apparently higher when compared to the GNF, GNF–PS, and GNF–TS.

Table 3. Antibacterial activity of the GNF and its PS and TS bionanocomposites, with 5% GNF, in comparison with the control.

Samples	Minimum Inhibitory Concentration (μg/mL)			
	Bacillus cereus	*Escherichia coli*	*Staphylococcus aureus*	*Salmonella typhimurium*
GNF	14 ± 2	13 ± 1	18 ± 0	31 ± 0
GNF–PS	9.1 ± 1	8.1 ± 1	15 ± 1	24 ± 2
GNF–TS	8.3 ± 1	3.1 ± 0	12 ± 2	19 ± 1
Positive Control	1.6 ± 0	0.4 ± 0	6 ± 0	12 ± 1

Values are expressed as the mean ± the standard error of mean (SEM), for triplicate readings.

4. Conclusions

The results presented here show that the incorporation of the cellulose nanofibers, extracted from ginger biomass, after the extraction of active constituents, and the prepared starch-based films were feasible in the production of nanocomposites through the solvent-casting method, and featured improved physiochemical properties. The combination of the PS and the TS starches (as the polymer matrix) and the GNF (as fillers for reinforcement purposes) was shown to possibly lead to nanocomposite films with superior barrier and mechanical properties. Mechanical properties, such as tensile strength and the elastic modulus were increased by the addition of 5% GNF concentrations to the starches. SEM analysis revealed the facilitation of bionanocomposites, which were dense structures with a large aggregation of tightly-packed GNF, due to the formation of new hydrogen bonds by the GNF, among the hydroxyl groups of the PS and the TS. XRD and FTIR data also revealed that the characteristic peak of the GNF indicated the incorporation of GNF in the bionanocomposite matrices. The antibacterial activities showed that the prepared-bionanocomposites exhibited good antibacterial performance against *Bacillus cereus*, *Escherichia coli*, *Staphylococcus aureus*, and *Salmonella typhimurium*, due to the addition of the GNF in the biopolymer matrixes.

The production of cellulose nanofibers from this underutilized agro-waste has the potential for commercial applications that could add value to ginger cultivation, generate extra income for farmers, and help in agribusiness diversification. In addition, the reuse of these residues allows a significant reduction, both, in the volume of waste accumulated in the environment and in the extraction of raw materials. Thus, the developed composite material could also be utilized for construction of packing materials, breathable wound dressing, surgical gloves, surgical gowns or drapes, medical bags, organ retrieval bags, and medical disposables.

Author Contributions: J.J. and S.G. did the conceptualization and methodology; J.J. and G.P. prepared and analyzed the GNF and composites; J.T.H. and S.T. did the supervision and project administration; J.J. prepared the manuscript and S.G. reviewed and edited.

Funding: This research received no external funding.

Conflicts of Interest: The authors declare no conflicts of interest.

References

1. Thompson, R.C.; Moore, C.J.; vom Saal, F.S.; Swan, S.H. Plastics, the environment and human health: Current consensus and future trends. *Philos. Trans. R. Soc. Lond. B Biol. Sci.* **2009**, *364*, 2153–2166. [CrossRef] [PubMed]
2. Jacob, J.; Haponiuk, J.T.; Thomas, S.; Gopi, S. Biopolymer based nanomaterials in drug delivery systems: A review. *Mater. Today Chem.* **2018**, *9*, 43–55. [CrossRef]
3. Mishra, R.K.; Ha, S.K.; Verma, K.; Tiwari, S.K. Recent progress in selected bio-nanomaterials and their engineering applications: An overview. *J. Sci. Adv. Mater. Dev.* **2018**, *3*, 263–288. [CrossRef]

4. Pelissari, F.M.; Andrade-Mahecha, M.M.; Sobral, P.J.D.A.; Menegalli, F.C. Nanocomposites based on banana starch reinforced with cellulose nanofibers isolated from banana peels. *J. Colloid Interface Sci.* **2017**, *505*, 154–167. [CrossRef] [PubMed]
5. Babu, R.P.; O'Connor, K.; Seeram, R. Current progress on bio-based polymers and their future trends. *Prog. Biomater.* **2013**, *2*, 8. [CrossRef] [PubMed]
6. Siro, I.; Plackett, D. Microfibrillated cellulose and new nanocomposite materials: A review. *Cellulose* **2010**, *17*, 459–494. [CrossRef]
7. Brinchi, L.; Cotana, F.; Fortunati, E.; Kenny, J.M. Production of nanocrystalline cellulose from lignocellulosic biomass: Technology and applications. *Carbohydr. Polym.* **2013**, *94*, 154–169. [CrossRef] [PubMed]
8. Samir, A.M.A.; Alloin, F.; Dufresne, A. Review of recent research into cellulosic whiskers, their properties and their application in nanocomposite field. *Biomacromolecules* **2005**, *6*, 612–626. [CrossRef] [PubMed]
9. Mishra, R.K.; Sabu, A.; Tiwari, S.K. Materials chemistry and the futurist eco-friendly applications of nanocellulose: Status and prospect. *Saudi Chem. Soc.* **2018**, in press. [CrossRef]
10. Gopi, S.; Amalraj, A.; Varma, K.; Jude, S.; Reddy, P.B.; Divya, C.; Haponiuk, J.T.; Thomas, S. Turmeric nanofiber-encapsulated natural product formulation act as a phytogenic feed additive—A study in broilers on growth performance, biochemical indices of blood, and *E. coli* in cecum. *Int. J. Polym. Mater. Polym. Biomater.* **2018**, *67*, 581–588. [CrossRef]
11. Gopi, S.; Amalraj, A.; Jude, S.; Varma, K.; Sreeraj, T.R.; Haponiuk, J.T.; Thomas, S. Preparation, characterization and anti-colitis activity of curcumin-asafoetida complex encapsulated in turmeric nanofiber. *Mater. Sci. Eng. C* **2017**, *81*, 20–31. [CrossRef] [PubMed]
12. Amalraj, A.; Jude, S.; Varma, K.; Jacob, J.; Gopi, S.; Oluwafemi, O.S.; Thomas, S. Preparation of a novel bioavailable curcuminoid formulation (Cureit™) using Polar-Nonpolar-Sandwich (PNS) technology and its characterization and applications. *Mater. Sci. Eng. C* **2017**, *75*, 359–367. [CrossRef] [PubMed]
13. Gopi, S.; George, R.; Thomas, M.; Jude, S. A pilot cross-over study to assess the human bio availability of "Cureit" A bio available curcumin in complete natural matrix. *Asian J. Pharm. Technol. Innov.* **2015**, *3*, 92–96.
14. Gopi, S.; Amalraj, A.; Jacob, J.; Kalarikkal, N.; Thomas, S.; Guo, Q. Preparation, characterization and in vitro study of liposomal curcumin powder by cost effective nanofiber weaving technology. *New J. Chem.* **2018**, *42*, 5117–5127. [CrossRef]
15. Prakobna, K.; Galland, S.; Berglund, L.A. High-performance and moisture-stable cellulose–starch nanocomposites based on bioinspired core–shell nanofibers. *Biomacromolecules* **2015**, *16*, 904–912. [CrossRef] [PubMed]
16. Dufresne, A.; Dupeyre, D.; Vignon, M.R. Cellulose microfibrils from potato tuber cells: Processing and characterization of starch–cellulose microfibril composites. *J. Appl. Polym. Sci.* **2000**, *76*, 2080–2092. [CrossRef]
17. Lobmann, K.; Svagan, A.J. Cellulose nanofibers as excipient for the delivery of poorly soluble drugs. *Int. J. Pharm.* **2017**, *533*, 285–297. [CrossRef] [PubMed]
18. Khoshnevisan, K.; Maleki, H.; Samadian, H.; Shahsavari, S.; Sarrafzadeh, M.H.; Larijani, B.; Dorkoosh, F.A.; Haghpanah, V.; Khorramizadeh, M.R. Cellulose acetate electrospun nanofibers for drug delivery systems: Applications and recent advances. *Carbohydr. Polym.* **2018**, *198*, 131–141. [CrossRef] [PubMed]
19. Worldatlas Canada. The Leading Ginger Producing Countries in the World. 1994. Available online: https://www.worldatlas.com/articles/the-leading-ginger-producing-countries-in-the-world.html (accessed on 25 April 2017).
20. Nafchi, A.M.; Moradpour, M.; Saeidi, M.; Alias, A.K. Thermoplastic starches: Properties, challenges, and prospects. *Starch* **2013**, *65*, 61–72. [CrossRef]
21. Vieira, M.G.A.; da Silva, M.A.; dos Santos, L.O.; Beppu, M.M. Natural-based plasticizers and biopolymer films: A review. *Eur. Polym. J.* **2011**, *47*, 254–263. [CrossRef]
22. Khan, B.; Niazi, M.B.K.; Jahan, G.S.Z. Thermoplastic starch: A possible biodegradable food packaging material—A Review. *J. Food Process Eng.* **2017**, *40*, e12447. [CrossRef]
23. Gutierrez, T.J.; Alvarez, V.A. Cellulosic materials as natural fillers in starch-containing matrix-based films: A review. *Polym. Bull.* **2017**, *74*, 2401–2430. [CrossRef]
24. Satyanarayana, K.G.; Prasad, V.S. Starch-based "Green" composites. In *Biodegradable Green Composites*, 1st ed.; Kalia, S., Ed.; John Wiley & Sons Inc.: Hoboken, NJ, USA, 2016; pp. 199–298.
25. Alam, M.N.; Christopher, L.P. A novel, cost-effective and eco-friendly method for preparation of textile fibers from cellulosic pulps. *Carbohydr. Polym.* **2017**, *173*, 253–258. [CrossRef] [PubMed]

26. Roilo, D.; Maestri, C.A.; Scarpa, M.; Bettotti, P.; Checchetto, R. Gas barrier and optical properties of cellulose nanofiber coatings with dispersed TiO_2 nanoparticles. *Surf. Coat. Technol.* **2018**, *343*, 131–137. [CrossRef]
27. Campano, C.; Merayo, N.; Negro, C.; Blanco, A. In situ production of bacterial cellulose to economically improve recycled paper properties. *Int. J. Biol. Macromol.* **2018**, *118*, 1532–1541. [CrossRef] [PubMed]
28. Pelissari, F.M.; Sobral, P.J.D.A.; Menegalli, F.C. Isolation and characterization of cellulose nanofibers from banana peels. *Cellulose* **2014**, *21*, 417–432. [CrossRef]
29. Kalita, D.; Kaushik, N.; Mahanta, C.L. Physicochemical, morphological, thermal and IR spectral changes in the properties of waxy rice starch modified with vinyl acetate. *J. Food Sci. Technol.* **2014**, *51*, 2790–2796. [CrossRef] [PubMed]
30. Oleyaei, S.A.; Almasi, H.; Ghanbarzadeh, B.; Moayedi, A.A. Synergistic reinforcing effect of TiO_2 and montmorillonite on potato starch nanocomposite film: Thermal, mechanical and barrier properties. *Carbohydr. Polym.* **2016**, *152*, 253–262. [CrossRef] [PubMed]
31. Deng, Z.; Jung, J.; Zhao, Y. Development, characterization and validation of chitosan absorbed cellulose nanofiber (CNF) films as water resistant and antibacterial food contact packing. *LWT–Food Sci. Technol.* **2017**, *83*, 132–140. [CrossRef]
32. Niu, X.; Liu, Y.; Song, Y.; Han, J.; Pan, H. Rosin modified cellulose nanofiber as a reinforcing and co-antimicrobial agents in polylactic acid/chitosan composite film for food packaging. *Carbohydr. Polym.* **2018**, *183*, 102–109. [CrossRef] [PubMed]
33. Llanos, J.H.R.; Tandini, C.C. Preparation and characterization of bio-nanocomposite film based on cassava starch or chitosan, reinforced with montmorillonit or bamboo nanofibers. *Int. J. Biol. Macromol.* **2018**, *107*, 371–382. [CrossRef] [PubMed]
34. Silverajah, V.S.; Ibrahim, N.A.; Zainuddin, N.; Yunus, W.M.; Hassan, H.A. Mechanical, thermal and morphological properties of poly(lactic acid)/epoxidized palm olein blend. *Molecules* **2012**, *17*, 11729–11747. [CrossRef] [PubMed]
35. Chundawat, S.P.; Bellesia, G.; Uppugundla, N.; da Costa, S.L.; Gao, D.; Cheh, A.M.; Agarwal, U.P.; Bianchetti, C.M.; Phillips, G.N., Jr.; Langan, P.; et al. Restructuring the crystalline cellulose hydrogen bond network enhances its depolymerization rate. *J. Am. Chem. Soc.* **2011**, *133*, 11163–11174. [CrossRef] [PubMed]
36. Wunderlich, B. *Thermal Analysis*, 1st ed.; Academic Press Inc.: San Diego, CA, USA, 1990.